Scaling behaviour near jamming in random sequential adsorption*

B. Purvis[1], L. Reeve[2], J.A.D. Wattis[2] and Y. Mao[1]
[1] *School of Physics and Astronomy, University of Nottingham, University Park, Nottingham, NG7 2RD*
[2] *School of Mathematics, University of Nottingham, University Park, Nottingham, NG7 2RD*
(Dated: January 22, 2015)

For the Random Sequential Adsorption model, we introduce the 'availability' as a new variable corresponding to the number of available locations in which an adsorbate can be accommodated. We investigate the relation of the availability to the coverage of the adsorbent surface over time. Power law scaling between the two is obtained both through numerical simulations and analytical techniques for both one and two dimensional RSA, as well as in the case of competitive random sequential adsorption in one dimension.

PACS numbers: 68.43.Mn Kinetics of adsorption
64.60.-i general studies of phase transitions
64.60.F- Equilibrium properties near critical points, critical exponents
64.60.fd General theory of critical region behavior

I. INTRODUCTION

The simplest case of Random Sequential Adsorption (RSA) in one dimension was developed by A. Rényi (1958) [1], and is sometimes known as the 'car parking problem'. In this model, one dimensional 'cars' of unit length are 'parked' sequentially at a random position on a continuous 'street' of length L. The cars are not allowed to overlap, and this parking process continues until there is no available space left in which to park, the point of jamming. Variations of Rényi's car parking problem include the effects of using a street of discrete units [2, 3], the use of a binary mixture of 'cars' or blocks of different lengths (Competitive Random Sequential Adsorption (CRSA)) [4–6], as well as extending the problem into higher dimensional space [7–10]. RSA and its variations have been used to model a wide range of physical phenomena, from protein adsorption [11], DNA charge neutralisation by polymers [12, 13], and polymer chain reactions [2], to catalysis [14], the nesting patterns of birds [15], and even election results [16].

In this paper, we report our finding of a power law scaling between the availability, defined as available locations for adsorption, and coverage. The paper is organized as follows. Section II describes one dimensional RSA using both discrete and continuous substrates. Section III extends this to the case of competitive RSA with two species of different lengths being adsorbed onto a one-dimensional substrate. In both cases we present numerical simulation results, showing power law scalings relating the availability to the coverage. The rationale for this power law scaling is derived from a theoretical analysis of the model of RSA, and supported by numerical simulations. Section IV examines the proposed power law relation in two dimensional systems, with our numerical simulations yielding scaling behaviour, albeit with different exponents. Finally, Section V provides discussions and observations, with suggestions for further research.

II. ONE COMPONENT RSA IN ONE DIMENSION

A common measure for parametrising RSA is the fraction of occupied sites, usually known as the coverage, $\theta(t)$. Many papers examine the coverage, and its evolution over time [1, 2, 6, 17]. Values of the final coverage $\theta(\infty)$ have been determined for various formulations of RSA, to varying degrees of accuracy, both analytically [1, 2] and through numerical simulations [17, 18]. In addition to the coverage, we shall define here another parameter which describes the total available space for adsorption. We call this parameter the availability, $A(t)$. For the discrete RSA model, we write this as

$$A(t) = \sum_{j=r}^{L} (j - r + 1) G_j(t), \tag{1}$$

where $G_j(t)$ is the gap distribution, that is, the number of gaps of length j present at time t. Noting that for blocks of length r, each gap of length $j \geq r$ yields a total of $j - r + 1$ available spots for adsorption.

For the one-dimensional continuum adsorption case, with blocks of unit length, the sum becomes an integral, with the length of gaps now defined by x and noting that in the continuum limit, each gap contains a space of $x - r$ for adsorption, we have

$$A(t) = \int_{x=r}^{L} (x - r) G(x, t) \, \mathrm{d}x. \tag{2}$$

The availability parameter represents the number of free sites where adsorption can occur, this is distinct from the sum of unoccupied sites. Whilst the difference between an unoccupied site and a site available for adsorption may

* Corresponding authors' emails: ppybp@nottingham.ac.uk, pmylr3@nottingham.ac.uk, Jonathan.Wattis@nottingham.ac.uk, Yong.Mao@nottingham.ac.uk, BP and LR contributed equally to this work.

be subtle, it is important: if, in the discrete case blocks of size $r > 1$ are being adsorbed, a single unoccupied site surrounded by occupied sites is not available for binding, where as a gap of length r allows one binding site and a gap of length $r + 1$ gives rise to two possible binding sites.

A. The discrete one component case in 1D

We now consider the discrete one-dimensional RSA process, and in particular its jamming limit. We measure the availability and coverage at each successful placement of a block. Numerical simulations have been run using two independently written programs, yielding excellent agreement in results. A logarithmic plot of scaled availability (1) against rescaled coverage is presented in Figure 1 as the dark solid line. A faint line of gradient one is displayed for comparison. For ease of comparison, instead of the coverage, θ, given by

$$\theta(t) = 1 - \frac{1}{L}\sum_{j=1}^{L} jG_j(t), \tag{3}$$

we use the scaled difference between final and current coverages, that is, $X/\theta(\infty)$ where

$$X = \theta(\infty) - \theta(t). \tag{4}$$

We also scale availability with its initial value, that is $A(t)/A(0)$, where $A(0) = L - r + 1$ as given by (1), corresponding to an empty street.

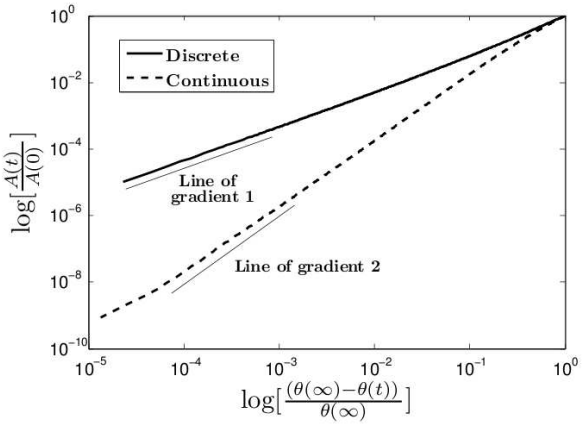

FIG. 1. Scaled $\log_{10}$-$\log_{10}$ plot of availability against coverage for a street of length 10^5. Landing blocks of length two on a discrete street (solid line), and blocks of unit length on a continuous street (dashed line). Each set of results is the average of 100 simulations.

As Figure 1 shows, the logarithmic plot of availability against coverage for the discrete street matches well with the line of unit gradient as coverage $\theta(t)$ approaches its maximum value of $\theta(\infty)$. Agreement within one standard deviation for three decades on the logarithmic (base 10) axes, provides strong evidence that as jamming is approached, there is a linear relation between availability and rescaled coverage, that is,

$$A(t) \propto \theta(\infty) - \theta(t). \tag{5}$$

This result can be interpreted as the rate of convergence to steady-state is determined by the binding of adsorbents of length r into gaps of length r, that is, the smallest available gaps are the last to be used as they are the hardest to find. That is, as $t \to \infty$, both A and X decrease to zero in proportion to each other as, in the final stages of adsorption, the gaps of r are the ones to be filled at the slowest rate, as longer gaps having been filled earlier in the process. The filling of a gap of size r causes A to reduce by $1/(L - r + 1)$ X to reduce by r/L.

B. Analysis of discrete 1D RSA

Turning to this same problem analytically we now show that such a power law scaling should be expected in the jamming limit.

As a preliminary to investigating this relation, we first determine a relation for the distribution of gaps, $G_j(t)$. We use the kinetic equations

$$\frac{\mathrm{d}G_j}{\mathrm{d}t} = -K_f(j + 1 - r)G_j, \quad (L - r + 1 \le j \le L), \tag{6}$$

$$\frac{\mathrm{d}G_j}{\mathrm{d}t} = -K_f(j + 1 - r)G_j + \sum_{p=j+r}^{L} 2K_f G_p, \quad (r \le j \le L - r), \tag{7}$$

$$\frac{\mathrm{d}G_j}{\mathrm{d}t} = \sum_{p=j+r}^{L} 2K_f G_p, \qquad (0 \le j \le r - 1), \tag{8}$$

presented in eq (5) of Maltsev *et al.*[12]; here, K_f is the rate at which the blocks land. The first of these equations describes the destruction of extremely large gaps, which occurs at the start of the binding process. The presence of the sink term in (7) is due to gaps which are destroyed as blocks land, and the source term describes the formation of new smaller gaps due to landing blocks.

In the large time limit, we make the ansatz that $G_j(t)$ has the form

$$G_j(t) = \begin{cases} \bar{G}_j - B_j(t), & (j = 0, 1, ..., r - 1), \\ \alpha \mathrm{e}^{(r-j-1)m(t)}, & (j = r, r + 1, ..., L - r), \end{cases} \tag{9}$$

where $B_j(t) \to 0$ as $t \to \infty$.

We differentiate the ansatz (9) and equate it to (7) to obtain

$$\frac{\mathrm{d}m}{\mathrm{d}t} = K_f + \frac{1}{r - j - 1}\sum_{p=j+r}^{L} 2K_f \mathrm{e}^{(j-p)m(t)}. \tag{10}$$

We are interested in the state of the substrate close to jamming, where $t \gg 1$, and consequently $m \gg 1$. In this limit, the sum in (10) can be neglected as it is asymptotically small in comparison to the other terms. This leaves $\mathrm{d}m/\mathrm{d}t = K_f$, which implies

$$m(t) = K_f t. \tag{11}$$

We now use the ansatz solution (9) with (11) to approximate the availability A, and coverage θ in the approach to jamming. In the limit $t \to \infty$, we have $m \gg 1$,

$$A(t) = \sum_{j=r}^{L} (j - r + 1) G_j(t) \sim \alpha \mathrm{e}^{-m(t)}. \tag{12}$$

Since

$$\theta(t) = 1 - \frac{1}{L}\sum_{j=1}^{r-1} j\bar{G}_j + \frac{1}{L}\sum_{j=1}^{r-1} jB_j(t) - \frac{1}{L}\sum_{j=r}^{L} \alpha j \mathrm{e}^{(r-1-j)m(t)}, \tag{13}$$

and $\theta(\infty) = 1 - (1/L)\sum_{j=1}^{r-1} j\bar{G}_j$, the difference X, defined by equation (4), is given by

$$X(t) = \frac{1}{L}\sum_{j=r}^{L} \alpha j \mathrm{e}^{(r-j-1)m(t)} - \frac{1}{L}\sum_{j=1}^{r-1} jB_j(t). \tag{14}$$

where, using the ansatz (9), the first sum corresponds to gaps of length $j \geq r$, and the second sum is due to correction terms in the distribution of gaps of length $j < r$. In the Appendix we justify neglecting $B_j(t)$ in the large-time limit.

Since the first in (14) dominates the second, we approximate (14) by

$$X = \frac{\alpha r e^{-m}}{L}. \tag{15}$$

Thus, combining (12) and (15), we have

$$A(t) \propto \theta(\infty) - \theta(t), \tag{16}$$

near jamming, confirming the power law in Figure 1.

C. Continuous RSA in 1D

We use a continuous street akin to that used in Rényi's original parking problem [1]. In place of (3), the coverage is now defined by

$$\theta(t) = 1 - \frac{1}{L}\int_{x=0}^{L} xG(x,t)\,\mathrm{d}x. \tag{17}$$

As should be expected, the total coverage, $\theta(\infty)$, is greater than in the discrete case, and our simulations matched the established value [19] of Rényi's parking constant to four decimal places. For the continuous case, we define the availability by assigning each gap of size $x > r$ an availability density proportional to $x - r$ and summing over all possible gaps $x > r$, hence

$$A(t) = \int_{x=r}^{L} (x - r) G(x,t)\,\mathrm{d}x. \tag{18}$$

Running our simulation 100 times for a street of length $L = 10^5$ we were able to calculate a mean value line for the availability as a function of coverage, which is plotted in a $\log_{10}$–$\log_{10}$ plot as the dashed line in Figure 1. As Figure 1 shows, this gradient has the value two, across three horizontal decades, in the approach to jamming, suggesting a power law relation of

$$A(t) \propto [\theta(\infty) - \theta(t)]^2. \tag{19}$$

D. Analysis of continuous RSA in 1D

Using a similar approach to that used in the discrete case, we show that this power law scaling of exponent 2 close to jamming is expected. Examining first the gap distribution in the case of continuous gap lengths described by x, the governing kinetic equations are given by

$$\frac{\partial G}{\partial t} = -K_f(x - r)G(x,t), \qquad (L - r < x < L), \tag{20}$$

$$\frac{\partial G}{\partial t} = -K_f(x - r)G(x,t) + \int_{y=x+r}^{L} 2K_f G(y,t)\,\mathrm{d}y, \qquad (r < x < L - r), \tag{21}$$

$$\frac{\partial G}{\partial t} = \int_{y=x+r}^{L} 2K_f G(y,t)\,\mathrm{d}y, \qquad (0 < x < r). \tag{22}$$

Solving (21) using the ansatz

$$G(x,t) = \begin{cases} \alpha \mathrm{e}^{(r-x)m(t)} & (r < x < L - r) \\ \overline{G}(x) - B(x,t) & (x < r) \end{cases} \tag{23}$$

yields

$$\frac{\mathrm{d}m}{\mathrm{d}t} = K_f - \frac{2K_f[\mathrm{e}^{-rm(t)} - \mathrm{e}^{-(L-x)m(t)}]}{(x - r)m(t)}. \tag{24}$$

Since $m \gg 1$ in the limit $t \to \infty$, the second term on the right hand side is negligible, giving $m(t) = K_f t$, which is the same solution as in the discrete case, namely (11).

Using the solution ansatz (23) for $G(x,t)$ together with (4) and (17), we find

$$X = \frac{1}{L}\int_{x=r}^{L} xG(x,t)\,\mathrm{d}x - \frac{1}{L}\int_{x=0}^{r} xB(x,t)\,\mathrm{d}x. \tag{25}$$

It can been shown that the contribution of the term involving $B(x,t)$ is negligible (see the Appendix for more details), thus (25) can be approximated by

$$X(t) = \frac{\alpha r}{Lm(t)} + \mathcal{O}(m(t)^{-2}). \tag{26}$$

More simply, the availability (18) is given by

$$A(t) = \int_{x=r}^{L} (x-r)G(x,t)\,\mathrm{d}x \sim \frac{\alpha}{m(t)^2}. \tag{27}$$

Taking the leading order term of (26), as $m \gg 1$, we arrive at the relation $A \propto X^2$ consistent with the straight line with gradient 2 observed in Figure 1.

III. TWO COMPONENT RSA IN ONE DIMENSION

Competitive Random Sequential Adsorption involves the random sequential adsorption of two components of differing lengths, which we label r and s respectively, where $r < s$. Various studies of competitive RSA exist in the literature, with analytical results for both gap distribution and coverage [5, 6, 13, 20–22]. In our investigations of CRSA, we continue to focus on the relationship between coverage and availability and the effect of adding a second component has on this relationship. A more detailed analysis of this problem is presented in [23]. We start with the discrete formulation and later consider the continuous version. We then present the results from our simulations, discussing the similarities and differences in behaviour.

A. Discrete two component RSA in 1D

For the two component case, the equations governing the evolution of the distribution of gap sizes have to be revised. For intermediate sizes we have

$$\frac{\mathrm{d}G_j}{\mathrm{d}t} = -K_r(j+1-r)G_j - K_s(j+1-s)G_j + 2K_r\sum_{p=j+r}^{L} G_p + 2K_s\sum_{p=j+s}^{L} G_p, \quad (s \le j < L-s), \tag{28}$$

$$\frac{\mathrm{d}G_j}{\mathrm{d}t} = -K_r(j+1-r)G_j + \sum_{p=j+r}^{L} 2K_rG_p + \sum_{p=j+s}^{L} 2K_sG_p, \quad (r \le j < s), \tag{29}$$

where K_r and K_s are the rates of adsorption of the r- and s-blocks respectively. The first sink term describes the loss of gaps of size j due to r-blocks landing, and the first source term describes the gain of gaps of size j due to an r-block landing. The latter sink and source terms follow from an s-block landing. Since the latter kinetic equation is for smaller gaps, there is no loss term for the binding of the s species. Other equations govern the destruction of gaps of sizes $L-s \le x \le L$, however, in the large time limit that we are concerned with here, it is reasonable to assume that no gaps of such large sizes are present.

As the governing equations for the distribution of gaps differs in the ranges $0 \le j < r$, $r \le j < s$ and $s \le j < L$ so does the solution for $G_j(t)$. However, the solutions can be obtained in the manner described in Section II B, yielding

$$G_j(t) = \begin{cases} \alpha \mathrm{e}^{-t[K_r(j+1-r)+K_s(j+1-s)]}, & (j \ge s), \\ \beta \mathrm{e}^{-tK_r(j+1-r)}, & (r \le j < s), \\ \bar{G}_j - B_j(t), & (1 \le j < r). \end{cases} \tag{30}$$

We now turn to investigate the relationship between $X(t) = \theta(\infty) - \theta(t)$ and the availability in the discrete CRSA. Following a similar method to the 1 component RSA, we write $X(t) = X_0(t) + X_1(t) + X_2(t)$ where

$$X_1(t) = \frac{1}{L}\sum_{j=r}^{s-1} jG_j(t) \sim \frac{\tilde{\beta}r}{L}e^{-K_rt}, \tag{31}$$

this simplification relying on $t \gg 1$. The first term is given by

$$X_0(t) = \sum_{j=1}^{r-1}(jG_j(t) - jG_j(\infty)) = -\sum_{j=1}^{r-1} jB_j(t), \tag{32}$$

which is smaller than X_1 in the large time limit (that is, $X_0 \ll X_1$). The third term is given by

$$X_2 = \frac{1}{L}\sum_{j=s}^{L} jG_j \sim e^{-t[K_s+(s-r+1)K_r]}. \tag{33}$$

with the simplification again relying on $L \gg 1$ and $t \gg 1$. Since $X_2 \ll X_1$ we have $X \sim X_1$ given by (31).

We now consider the availability, $A(t)$, noting that the availability for the longer block is different from that for the shorter, hence we require two availability parameters. We denote these as A_r for the availability of the short r-block and A_s for the availability of the longer s-block. For the shorter block, we have

$$A_r = \frac{1}{L}\sum_{j=r}^{s-1}(j-r+1)G_j + \frac{1}{L}\sum_{j=s}^{L}(j-r+1)G_j, \tag{34}$$

Inserting our previously defined relations for the gap distribution, (30) into (34) and retaining only the leading order terms, we obtain

$$A_r \sim \frac{\beta e^{-K_rt}}{L}. \tag{35}$$

The availability for the longer block is given by

$$A_s = \frac{1}{L}\sum_{j=s}^{L} G_j(j-s+1) \sim \frac{1}{L}\alpha e^{-t[K_s+K_r(s+1-r)]}. \tag{36}$$

Combining (31), (35) and (36) we find

$$A_r \propto X, \qquad A_s \propto X^{1+s-r+K_s/K_r}. \tag{37}$$

B. Continuous two-component RSA in 1D

In the continuous case, the distribution of gaps $G(x,t)$ changes considerably from (21); the evolution of the distribution is now determined by

$$\frac{\partial G}{\partial t} = -(x-r)K_r G(x,t) - (x-s)K_s G(x,t) + 2K_r \int_{x+r}^{L} G(y,t)\,\mathrm{d}y + 2K_s \int_{x+s}^{L} G(y,t)\,\mathrm{d}y, \quad (s < x < L-s), \tag{38}$$

$$\frac{\partial G}{\partial t} = -(x-r)K_r G(x,t) + 2K_r \int_{y=x+r}^{L} G(y,t)\,\mathrm{d}y + 2K_s \int_{x+s}^{L} G(y,t)\,\mathrm{d}y, \quad (r < x < s), \tag{39}$$

$$\frac{\partial G}{\partial t} = 2K_r \int_{x+r}^{L} G(y,t)\,\mathrm{d}y + 2K_s \int_{x+s}^{L} G(y,t)\,\mathrm{d}y, \quad (x < r), \tag{40}$$

together with other equations governing the evolution of gaps of sizes $L-s < x \le L$; however, since we are concerned with the transition to jamming, and extremely long gaps such as these are rapidly destroyed at the start of the adsorption, we will assume such large gaps can be neglected.

Due to the evolution equations (38)–(40), being more complicated than (28)–(29), it is necessary to modify the solution ansatz (30) also, to

$$G(x,t) = \begin{cases} \alpha e^{(\gamma - x)m(t)} & (x > s), \\ \beta e^{(\eta - x)n(t)} & (r < x < s), \\ \bar{G}(x) - B(x,t) & (x < r). \end{cases} \tag{41}$$

Considering first the larger gaps, of size $x > s$, from (38) and (41) we obtain

$$(\gamma - x)\frac{\mathrm{d}m}{\mathrm{d}t} = rK_r - xK_r + sK_s - xK_s, \tag{42}$$

hence $\gamma = (rK_r + sK_s)/(K_r + K_s)$, $m(t) = (K_r + K_s)t$ and

$$G(x,t) = \alpha e^{-t[K_r(x-r) + K_s(x-s)]}, \quad (x > s). \tag{43}$$

For gaps of length $r \le x < s$, we obtain $(\eta - x)\mathrm{d}n/\mathrm{d}t = K_r(r-x)$, so $\eta = r$, $n(t) = K_r t$ and

$$G(x,t) = \beta e^{-K_r t(x-r)}, \quad (r \le x < s). \tag{44}$$

To investigate the self similarity in the continuous case, we recall the definition $X = \theta(\infty) - \theta(t)$, which can be calculated from

$$X(t) = \frac{1}{L}\int_r^s xG(x,t)\,\mathrm{d}x + \frac{1}{L}\int_s^L xG(x,t)\,\mathrm{d}x. \tag{45}$$

In the large time limit, the dominant terms arise from the first integral, and lead to

$$X \sim \frac{\beta r}{tK_r} + \frac{\beta}{t^2 K_r^2}, \tag{46}$$

with the latter integral being exponentially small in t.

As in the discrete case, there are two availabilities, A_r and A_s defined respectively by

$$A_r(t) = \frac{1}{L}\int_r^L (x-r)G(x,t)\,\mathrm{d}x, \tag{47}$$

$$A_s(t) = \frac{1}{L}\int_s^L (x-s)G(x,t)\,\mathrm{d}x. \tag{48}$$

Substituting solution (41) into (48) and expanding for the limit $t \gg 1$ leads to

$$A_r(t) \sim \frac{\beta}{t^2 K_r^2} + \mathcal{O}(t^{-1}\mathrm{e}^{-tK_r(s-r)}), \tag{49}$$

$$A_s(t) \sim \frac{\alpha \mathrm{e}^{-tK_r(s-r)}}{(K_r + K_s)^2 t^2}. \tag{50}$$

Comparing (49) and (50) with (46) we note that $A_r \sim X^2$, the same power law scaling as in the single component case of RSA; however, the availability for the longer block decays exponentially, being given by $A_s \sim X^2 \mathrm{e}^{-\kappa/X}$ for some κ, a quite different form to A_s given by (37).

C. Numerical simulations of two component RSA in 1D

Summarising briefly our results from mathematical analysis, we have, for the discrete and continuous cases respectively

$$A_{r,\mathrm{disc}} = \gamma_{r,d} X, \text{ and } A_{s,\mathrm{disc}} = \gamma_{s,d} X^{1+s-r+K_s/K_r}, \tag{51}$$

$$A_{r,\mathrm{cts}} = \gamma_{r,c} X^2, \text{ and } A_{s,\mathrm{cts}} = \gamma_{s,c} X^2 \mathrm{e}^{-\gamma(s-r)/X}. \tag{52}$$

Thus, on a $\log_{10}$-$\log_{10}$ plot, we expect straight lines with gradient one and two for the availability of the shorter species, $A_{r,\mathrm{disc}}$, $A_{r,\mathrm{cts}}$, in the discrete and continuous cases respectively, a result equal to the one component case. For the availability of the larger block, A_s, the relationship is more complicated. For the discrete case, we expect a linear relation with gradient $1 + s - r + K_s/K_r$, which becomes increasingly steep as the ratio of s to r becomes more extreme, and as the relative rate of adsorption K_r/K_s increases. However, for the continuous case, our theory does not produce such a simple expression; rather a much more rapid decay of A to zero as $X \to 0$.

Figure 2 shows the results of numerical simulations of both discrete and continuous CRSA. The simulation provides strong evidence for the power law relation for the availability of the shorter species, r, in both continuous and discrete cases. The small differences between our simulations and the theory at the lower extremes of the graph presented above are due to infrequent sampling of this limit. The relationship governing the availability of the longer species, s, is more difficult to determine from the plot. The simulation results for A_s in the discrete

case match well to a straight line of gradient 10, as predicted by our theoretical calculations. We observe in Figure 2 that the curves corresponding to A_s in the discrete and continuous cases are fairly similar. Even though the formulae (51) and (52) for A_s differ between the discrete and continuous cases, both formulae predict extremely rapid decay in A_s as X decreases to zero.

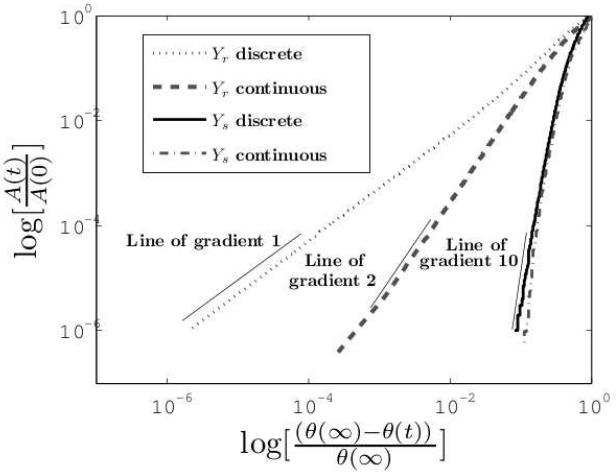

FIG. 2. Log_{10}-$\log_{10}$ plot of availability against coverage showing the average of 100 simulations for both discrete and continuous CRSA, with blocks of sizes $r = 2$ and $s = 10$ binding with equal probabilities on a substrate of length $L = 10^5$.

In order to verify (52), we plot $\log_{10}(A_{s,cts}/X^2)$ against $1/X$ in Figure 3. This shows an approximately linear relationship between the rescaled availability and $1/X$ as $1/X$ increases from 2.5 to 7, which corresponds to the remaining coverage X decreasing from 0.4 to 0.14. At lower values of X, ($X < 0.18$, corresponding to $1/X > 5.5$) there is rarely any availability for the longer blocks, and we observe significant fluctuations, which would only be removed by averaging over a much higher number of simulations.

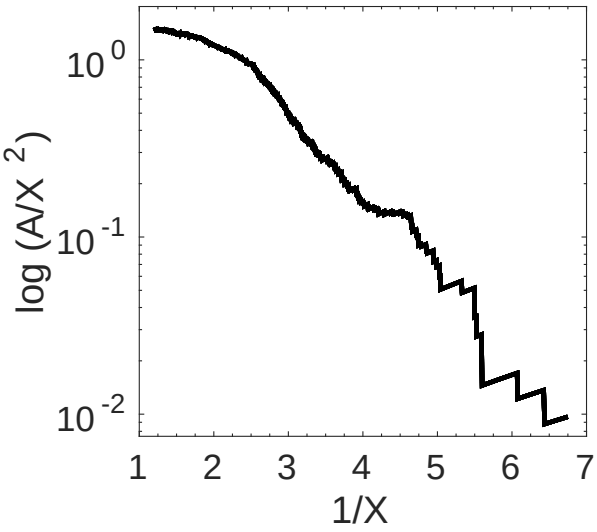

FIG. 3. Plot of $\log_{10}(A_{s,cts}/X^2)$ against $1/X$ for the average of 100 simulations for the case of CRSA on a continuous substrate, with blocks of sizes $r = 2$ and $s = 10$ binding with equal probabilities to a substrate of length $L = 10^5$.

IV. SIMULATIONS OF RSA IN TWO DIMENSIONS

Adding a second spatial dimension introduces additional levels of complexity, and much of the analytical techniques become non-trivial [24, 25]. Due to this, the study of RSA in two dimensions has been largely confined to the use of computer simulations [17, 18, 26]. Various approaches have modelled the two-dimensional blocks as rectangles [27], discs [17, 26], squares [25], and more complex asymmetric shapes, or 'Lattice Animals' [8].

In our approach we generalise the two-dimensional blocks to squares with side of length n, and modelled their adsorption onto a discrete square lattice with sides of length N. We tested both solid (impenetrable) and periodic boundary conditions, and determined that for a sufficiently large lattice, no noticeable difference in the coverage or availability was observed; we therefore decided to use solid boundary conditions as these codes required less processing power.

It should be noted that in our two-dimensional simulations, the coverage, $\theta(t)$, is again defined as the fraction of filled sites to empty sites; thus if Z blocks have bound to the substrate, the coverage θ is given by $\theta = Zn^2/N^2$. The two-dimensional availability, $A(t)$, is defined as the number of sites where there is an $r \times r$ unoccupied space, i.e. where there is available place for a block to bind. Clearly this is more difficult to simulate than the one-dimensional case, and the theoretical analysis of this case is also significantly more complicated, so will not be attempted here.

In our initial simulation we landed 2×2 square blocks ($n = 2$) on lattices of various size, before settling on an $N = 5000$ which we deemed to be adequately large. This configuration resulted in a final coverage, $\theta(\infty)$, of approximately 0.748.

Creating an algorithm to simulate RSA onto a continuous two-dimensional surface has been explored in the last few decades [17, 18, 26]. The main challenge lies in locating those sites which remain available for adsorption; as the jamming limit is approached, the size of such sites reduces, and form a vanishingly small proportion of the total substrate. Various approaches initially simulate a continuous substrate and later switch to a discrete lattice when close to jamming, increasing the resolution after each successful placement [18, 26]. Due to processing constraints, and the fact that calculating the availability for a continuous surface presents additional difficulties,

we have modelled the continuum limit by increasing the size of the adsorbing square blocks n. The results of this approach to the continuum limit are shown in Figure 4, culminating in the adsorption of square blocks with side length $n = 100$ on a square substrate of side length $N = 10,000$. This configuration yields an average final coverage of $\theta(\infty) = 0.5621$ agreeing within error of Cadilhe *et al.*'s value of 0.5620 for placement of squares on a continuous two dimensional square surface [9]. However, we note that this value differs from the approximation of Pálaste [28] cited by Feder [17] of $\theta_{2D} = \theta_{1D}^2$, which gives 0.5589 in the continuous case, a difference of 0.57%.

As can be seen in Figure 4, there is strong evidence that the two-dimensional RSA obeys the same power law scaling for the relation between coverage and availability as for the case of a one-dimensional substrate. The curve corresponding to $n = 2$, namely the discrete case has a gradient of unity close to jamming, suggesting that the relation of $A(t) \propto \theta(\infty) - \theta(t)$ holds, as in equation (16). As we consider larger values of n, the approach to a continuum limit is made, where the gradient is approximately two, as in the continuous one-dimensional case (19).

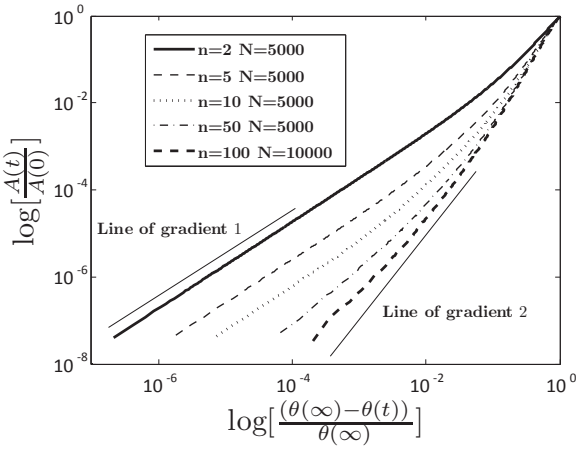

FIG. 4. Log_{10}-$\log_{10}$ plot of availability against coverage for a two-dimensional square lattice with sides upto length $N = 5000$ to show an approach to the continuum limit, each simulation was performed 5 times and a mean taken. The adhering blocks were also taken to be square, with sides of lengths $n = 2, 5, 10, 50$ and $n = 100$, and $N = 5000$ in all cases except the last, where $N = 10000$. Larger values of n illustrate results closer to the continuum limit.

V. DISCUSSION

We have introduced a new measure of the distance from the total jamming transition point, namely the 'Availability' of a partially-filled substrate. This has a valid definition in both discrete and continuous formulations of RSA, and in whatever dimension of substrate one chooses to consider. In systems with mixed species being adsorbed, there is an availability measure for each species, which we have illustrated using a two-component competitive RSA model in one dimension.

Defining the coverage deficit by $X(t) = \theta(\infty) - \theta(t)$, we have that both the availability $A(t) \to 0$ and the deficit $X(t) \to 0$ in the jamming limit, that is, as $t \to \infty$. The power law scaling relating availability A and X appear universal, with the power depending on the specific case of the RSA. For the simplest case of one block size binding to a substrate, we have, in the discrete case, $A(t) \sim X(t)$, whereas in the continuous case, $A(t) \sim (X(t))^2$. For the more complex case of competitive binding of two block lengths on a one-dimensional substrate, we have two availabilities; one for the short and the other for the long blocks. We again have $A_r(t) \sim X(t)$ and $A_r(t) \sim X(t)^2$ for the short blocks, in the discrete and continuous cases respectively; and different types of much more rapid decay for the longer species, specifically, $A_s(t) \sim X(t)^{1+s-r+K_s/Kr}$ and $A_s(t) \sim X(t)^2 \mathrm{e}^{-\kappa/X(t)}$ in the discrete and continuous cases respectively. For the one-dimensional cases, we have provided theoretical justification of these results via an analysis of the evolution of the gap distribution profile. In the case of two-dimensional species adsorbing onto a two-dimensional substrate, we find the same exponents, namely one for the discrete case ($A = X$) and two for the continuous ($A \sim X^2$). Whilst Feder's assumption that the limiting coverage should be the square of the one-dimensional case is a reasonable approximation, it should be noted that it is only an approximation, and simulations show a different result. The theory for the two-dimensional substrates remains an open problem, due to the difficulty in defining a quantity analogous to the gap distribution in the one-dimensional systems.

The universal power law scaling between availability and coverage could be significant. The availability clearly has implications for the rate of adsorption, and may be of particular relevance to cases such as catalysis. It would be interesting to investigate further cases of ellipsoidal or needle-like species adsorbing onto a two-dimensional substrate, or RSA in higher-dimensions to see if the power law scaling hold for more complex cases of RSA.

Acknowledgements

LR is grateful to the Wellcome Trust for a Vacation Research Bursary, and BP to the University of Nottingham Science Faculty Dean's fund for support. We thank the referees for their helpful suggestions.

Appendix A: Magnitudes of neglected terms

Here we present the detailed calculations supporting some of the more technical assertions made in the main body of the paper. These calculations show that terms neglected in the main calculations are indeed smaller than the retained terms, so justifying the approximations made.

1. Discrete 1D RSA

We show why the second term in (14) can be neglected. Using (8) and (9), together with $L \gg 1$ and the solution $m(t) = K_f t$, we obtain

$$\frac{\mathrm{d}B_j}{\mathrm{d}t} = -2K_f\alpha \sum_{p=j+r}^{L} \mathrm{e}^{m(r-p-1)} \tag{A1}$$

$$\sim -\frac{2K_f\alpha \mathrm{e}^{-m(j+1)}}{1-\mathrm{e}^{-m}} = -2K_f\alpha \mathrm{e}^{-(j+1)K_f t}. \tag{A2}$$

Hence, for $j < r$, $B_j(t) = 2\alpha \mathrm{e}^{-(j+1)K_f t}/(j+1)$ and so

$$\sum_{j=1}^{r-1} jB_j(t) = \sum_{j=1}^{r-1} \frac{2\alpha j \mathrm{e}^{-(j+1)K_f t}}{(j+1)}, \tag{A3}$$

which decays faster than $X \sim \mathrm{e}^{-m(t)} \sim \mathrm{e}^{-K_f t}$ as $t \to \infty$.

2. Continuous1D RSA

Turning to the continuous case, we now show why the second term in (25) can be ignored in the large-time limit. Using (22) and (23) we obtain

$$\frac{\partial B}{\partial t} = -2K_f\alpha \int_{y=x+r}^{L} \mathrm{e}^{m(r-y)}\,\mathrm{d}y$$

$$\sim -2\alpha K_f \mathrm{e}^{-mx} \int_{u=0}^{\infty} \mathrm{e}^{-mu}\mathrm{d}u$$

$$= \frac{-2\alpha K_f \mathrm{e}^{-mx}}{m} = \frac{-2\alpha \mathrm{e}^{-K_f x t}}{t}. \tag{A4}$$

While it is possible to integrate this expression, leading to $B(x,t) = 2\alpha Ei(K_f x t)$ where Ei is the exponential integral function, with details given in Olver *et al.* [29], it is simpler to leave $B(x,t)$ as an integral over t, then evaluate $\int_0^r xB\mathrm{d}x$ by changing the order of integration. Hence

$$\int_{x=0}^{r} xB(x,t)\mathrm{d}x = \int \frac{2\alpha r \mathrm{e}^{-K_f r t}}{K_f t^2} + \frac{2\alpha \mathrm{e}^{-K_f r t}}{K_f^2 t^3} - \frac{2\alpha}{K_f^2 t^3}\,\mathrm{d}t$$

$$= \frac{\alpha}{K_f^2 t^2} - \frac{2\alpha r \mathrm{e}^{-K_f r t}}{K_f t} + 2\alpha r^2 \mathrm{Ei}(K_f x t)$$

$$+ \frac{\alpha r \mathrm{e}^{-K_f r t}}{K_f t} - \frac{\alpha \mathrm{e}^{-K_f r t}}{K_f^2 t^2} - \alpha r^2 \mathrm{Ei}(K_f r t)$$

$$= \frac{\alpha}{K_f^2 t^2} + \mathcal{O}(t^{-1}\mathrm{e}^{-K_f}); \tag{A5}$$

and thus $\int_0^r xB\mathrm{d}x$ is smaller than X given by (26) by one power of t.

[1] A. Rényi, Publ. Math. Inst. Hung. Acad. Sci. **3**, 109-127, (1958).
[2] P. J. Flory, J. Am. Chem. Soc. **61**, 1518-1521, (1939).
[3] E. R. Cohen and H. Reiss, J. Chem. Phys. **38**, 680-691, (1963).
[4] J. P. Mullooly, J. Appl. Probab. **5**, 427-435, (1968).
[5] M. K. Hassan, J. Schmidt, B. Blasius and J. Kurths Phys. Rev. E. **65**, 045103, (2002).
[6] D. J. Burridge and Y. Mao, Phys. Rev. E. **69**, 037102, (2004).
[7] K. J. Vette, T. W. Orent, D. K. Hoffman and R. S. Hansen,J. Chem. Phys. **60**, 4854-4861, (1974).
[8] R. S. Nord and J. W. Evans J. Chem. Phys. **82**, 2795-2810, (1985).
[9] A. Cadilhe, N. A. M. Araùjo and V. Privman, J. Phys. Cond. Mat. **19**, 065124, (2007).
[10] B. Bonnier, M. Hontebeyrie and C. Meyers, Physica A. **198**, 1-10, (1993).
[11] P. Katira, A. Agarwal, H. Hess, Adv. Mater. **21**, 1599-1604, (2009).
[12] E. Maltsev, J. A. D. Wattis and H. M. Byrne, Phys. Rev. E. **74**, 011904, (2006).
[13] E. Maltsev, J. A. D. Wattis and H. M. Byrne, Phys. Rev. E. **74**, 041918, (2006).
[14] A. S. McLeod and L. F. Gladden, J. Chem. Phys. **110**, 4000-4008, (1999).
[15] M. Tanemura and M. Hasegawa, J. Theor. Biol. **82**, 477-496, (1980).
[16] Y. Itoh and S. Ueda Ann. Inst. Stat. Math. **31**, 157-167, (1979).
[17] J. Feder J. Theor. Biol. **87**, 237-254, (1980).
[18] S. Suh, B. Jung, Y. Park, V. Chihaia, V. Parvulescu and M. Gartner. Bull. Korean Chem. Soc. **29**, 873-875, (2008).
[19] S. R. Finch *Mathematical Constants* (Cambridge University Press, Cambridge, 2003) p.278.
[20] M. K. Hassan and J. Kurths J. Phys. A. **34**, 7517-7525, (2001).
[21] M. C. Bartelt and V. Privman Phys. Rev. A. **44**, R2227-R2230, (1991).
[22] N. A. M. Araújo, A. Cadilhe Phys. Rev. E. **73**, 051602 (2006).
[23] L. Reeve and J.A.D. Wattis. *submitted*, (2015).
[24] P. Schaaf and J. Talbot Phys. Rev. Lett. **62**, 175-178, (1989).
[25] P. Schaaf, J. Talbot, H. M. Rabeony, H. Reiss. J. Phys. Chem. **92**, 4826-4829, (1988).
[26] J.-S. Wang Int. J. Mod. Phys. C. **05**, 707-716, (1994).

[27] R. D. Vigil and R. M. Ziff. J. Chem. Phys. **91**, 2599-2602, (1989).
[28] A. Pálaste. Publ. Math. Inst. Hungar. Acad. Sci. **3**, 109, (1960).
[29] F. W. J. Olver, D. W. Lozier, R. F. Boisvert, and C. W. Clark, editors. NIST Handbook of Mathematical Functions. CUP, New York, NY, (2010). [also available at http://dlmf.nist.gov/6]